Deficiency in ethanolamine plasmalogen leads to altered cholesterol transport

Natalie J. Munn,* Emily Arnio,* Dailan Liu,† Raphael A. Zoeller,† and Laura Liscum[1,*]

Department of Physiology,* Tufts University School of Medicine, Boston, MA 02111; and Department of Physiology and Structural Biology,† Boston University School of Medicine, Boston, MA 02118

Abstract **Plasmalogens are a major sub-class of ethanolamine and choline phospholipids in which the *sn*-1 position has a long chain fatty alcohol attached through a vinyl ether bond. These phospholipids are proposed to play a role in membrane fusion-mediated events. In this study, we investigated the role of the ethanolamine plasmalogen plasmenylethanolamine (PlsEtn) in intracellular cholesterol transport in Chinese hamster ovary cell mutants NRel-4 and NZel-1, which have single gene defects in PlsEtn biosynthesis. We found that PlsEtn was essential for specific cholesterol transport pathways, those from the cell surface or endocytic compartments to acyl-CoA/cholesterol acyltransferase in the endoplasmic reticulum. The movement of cholesterol from the endoplasmic reticulum or endocytic compartments to the cell surface was normal in PlsEtn-deficient cells. Also, vesicle trafficking was normal in PlsEtn-deficient cells, as measured by fluid phase endocytosis and exocytosis, as was the movement of newly-synthesized proteins to the cell surface. The mutant cholesterol transport phenotype was due to the lack of PlsEtn, since it was corrected when NRel-4 cells were transfected with a cDNA encoding the missing enzyme or supplied with a metabolic intermediate that enters the PlsEtn biosynthetic pathway downstream of the defect. Future work must determine the precise role that plasmalogens have on cholesterol transport to the endoplasmic reticulum.—** Munn, N. J., E. Arnio, D. Liu, R. A. Zoeller, and L. Liscum. **Deficiency in ethanolamine plasmalogen leads to altered cholesterol transport. *J. Lipid Res.* 2003.** 44: **182–192.**

Supplementary key words plasmalogen • plasmenylethanolamine • cholesterol • somatic cell mutant

Plasmalogens are a major class of ethanolamine and choline phospholipids in which the *sn*-1 position of the glycerol backbone has a long chain fatty alcohol attached through a vinyl ether bond (1). They constitute 18% of total phospholipid mass in humans, with the highest amounts in heart, striated muscle, and nervous tissue (2). In the Chinese hamster ovary (CHO) cell line, 11% of the total phospholipids are plasmalogens, primarily ethanolamine plasmalogen, called plasmenylethanolamine (PlsEtn) (3). CHO cells do not contain plasmenylcholine (4). The cellular distribution of plasmalogens has not been thoroughly characterized, although they are reportedly present in plasma membrane (5), synaptic vesicles (6), and secretory granules (7). In erythrocytes, plasmalogens are found to be oriented with the same asymmetric distribution as their diacyl analogs (8).

For such an abundant phospholipid, plasmalogen functions are quite obscure. Current in vitro models suggest that PlsEtn plays a role in membrane fusion-mediated events (9) and protects against reactive oxygen species (10). In this study, we investigated the role of PlsEtn in cholesterol metabolism, prompted by the finding that cholesterol efflux to HDL is aberrant in plasmalogen-deficient RAW mutant macrophages (11). The lack of plasmalogens did not alter the rate of cellular cholesterol transfer to HDL; instead, it appeared to reduce the pool of cholesterol available for efflux. Another study showed that levels of PlsEtn are reduced in brain tissue from the Niemann-Pick C (NPC) mouse model (12). NPC cells exhibit lysosomal storage of cholesterol, gangliosides, and other lipids, as well as aberrant cholesterol homeostatic responses (13). If plasmalogens affect the cellular cholesterol distribution, then reduced plasmalogen levels might exacerbate the cholesterol transport defective phenotype of NPC and contribute to disease progression.

Our model systems were CHO cell mutants NRel-4 and NZel-1, which display greatly reduced levels of PlsEtn due to defects in different steps of plasmalogen biosynthesis (3, 14). NRel-4 has a defect in dihydroxyacetonephosphate acyltransferase (DHAPAT) (3), the enzyme that cat-

Manuscript received 11 September 2002 and in revised form 16 October 2002.

Published, JLR Papers in Press, November 4, 2002.
DOI 10.1194/jlr.M200363-JLR200

Abbreviations: CHO, Chinese hamster ovary; [^{3}H]CL-LDL, LDL that is labeled with [^{3}H]cholesteryl linoleate; DHAP, dihydroxyacetone phosphate; DHAPAT, dihydroxyacetone phosphate acyltransferase; ER, endoplasmic reticulum; HBSS, Hank's balanced salt solution; LPDS, lipoprotein-deficient serum; MTT, 3-(4,5-dimethyl thiazol-2-yl)-2,5-diphenyl tetrazolium bromide; NCS, newborn calf serum; NPC, Niemann-Pick disease type C; PlsEtn, plasmenyethanolamine.

[1] To whom correspondence should be addressed.
e-mail: laura.liscum@tufts.edu

alyzes the first step in plasmalogen biosynthesis. NZel-1 has a defect in alkyl-dihydroxyacetone phosphate (DHAP) synthase (14), which catalyzes the second step in plasmalogen biosynthesis.

Our analysis revealed that PlsEtn is essential for specific cholesterol transport pathways. In PlsEtn deficient cells, the movement of cholesterol from endocytic compartments or the plasma membrane to ACAT in the endoplasmic reticulum (ER) was deficient. Cholesterol movement to the plasma membrane appeared to be normal, as did vesicular protein trafficking. Defective cholesterol transport pathways were restored in NRel-4 cells transfected with a cDNA encoding the missing enzyme, DHAPAT, or supplied with an intermediate that enters the PlsEtn biosynthetic pathway downstream of the metabolic defect. These data support a role for PlsEtn in specific cholesterol transport pathways, those from the cell surface to the cell interior.

EXPERIMENTAL PROCEDURES

Materials

[9,10-^{3}H]oleic acid (5 Ci/mmol), [1-^{14}C]oleoyl-CoA (59 mCi/mmol), [1,2-^{3}H]cholesterol (45 Ci/mmol), [1,2,6,7-^{3}H]cholesteryl linoleate (75 Ci/mmol), [1,2,6,7-^{3}H]cholesteryl oleate (78 Ci/mmol), cholesteryl [1-^{14}C]oleate (57 mCi/mmol), [^{14}C(U)]sucrose (600 mCi/mmol), and EasyTag Express ^{35}S Protein Labeling Mix (1175 Ci/mmol) were obtained from NEN Life Science Products. Sodium ^{125}I (103 mCi/ml) was from Amersham Biosciences. Tissue culture reagents were from Life Technologies, Inc. or Sigma. Lipids were obtained from Sigma or Steraloids. Mevinolin was a generous gift of Merck Research Laboratory. Other chemicals were from Sigma unless otherwise indicated. Compounds were dissolved as follows: 25-hydroxycholesterol in ethanol, cholesterol in ethanol, and amphotericin B in dimethyl sulfoxide.

Cultured cells, preparation of LDL, lipoprotein-deficient serum, media, and buffers

LDL was prepared by ultracentrifugation (15). LDL labeled with [^{3}H]cholesteryl linoleate ([^{3}H]CL-LDL) was prepared with an average specific activity of 21,000 cpm/nmol of total cholesteryl linoleate (16). LDL labeled with [^{3}H]cholesteryl oleate ([^{3}H]CO-LDL) was prepared with an average specific activity of 38,000 dpm/nmol of total cholesteryl ester (16). ^{125}I-LDL was prepared by the iodine monochloride method (15). Lipoprotein-deficient serum (LPDS) was prepared as described, omitting the thrombin incubation (15). The following media were prepared: H-5% newborn calf serum (NCS) and H-10% NCS (Ham's F-12 medium containing 5% or 10% (v/v) newborn calf serum, 2 mM glutamine, 100 U/ml penicillin, 100 μg/ml streptomycin, and 20 mM HEPES, pH 7.1); H-5% LPDS and H-1% LPDS [H-5% NCS in which 5% (v/v) newborn calf serum was replaced with 5 or 1% (v/v) lipoprotein-deficient calf serum, respectively]; H-5% LPDS/mev (H-5% LPDS containing 20 μM mevinolin and 0.5 mM mevalonate).

The following buffers were prepared: TBS (50 mM Tris-Cl and 155 mM NaCl, pH 7.4) and PBS (1.5 mM KH_2HPO_4, 2.7 mM KCl, and 137 mM NaCl, pH 7.3).

All cells were grown as monolayers in a humidified incubator (5% CO_2) at 37°C in H-5% NCS. The mutant cell lines, NRel-4 (3) and NZel-1 (14), were isolated as described previously. NRel-4 and NZel-1 cells display deficiencies in DHAPAT and alkyl-DHAP synthase, respectively. Both show a 90% loss in PlsEtn levels compared with wild-type cells. NRel-4.15 is a clonal isolate, stably expressing human DHAPAT cDNA (kindly provided by Wilhelm Just, Univ. Heidelberg, and directionally inserted into the pBK-CMV expression vector; Stratagene) and containing wild-type plasmalogen levels. NRel-4.CMV has been transfected with vector alone and is plasmalogen-deficient (Zoeller et al., unpublished observations). CHO mutant 2-2 was isolated by Dahl et al. (17) and has the NPC phenotype. On day 0 of each experiment, monolayer stock flasks of CHO-K1 and mutant cells were trypsinized, and cells were seeded as indicated in the individual experiment.

Incorporation of [^{3}H]oleate into cholesteryl [^{3}H]oleate

On day 0, cells were seeded into 6-well plates (20,000 cells/well) in H-5% NCS. On day 2, cells were fed H-5% NCS. On day 3, cells were washed with Hank's balanced salt solution (HBSS) and fed H-5% LPDS. Experiments were conducted on day 4. Following additions of LDL or 25-hydroxycholesterol, monolayers were pulsed with 100 μM [^{3}H]oleate (prepared with a specific activity of 8,700 cpm/nmol) bound to albumin (15). After 2 h of [^{3}H]oleate incubation, cells were washed with TBS, lipids were extracted with hexane-isopropanol (3:2, v/v), and cholesterol [^{3}H]oleate was isolated and quantified (18). After lipid extraction, the monolayers were dissolved in 0.1 N NaOH and aliquots removed for protein determination (19) using BSA as a standard. Cholesterol esterification is defined as nmol [^{3}H]oleate incorporated into cholesteryl [^{3}H]oleate/h/mg protein.

ACAT assay in cell-free extracts

On day 0, cells were seeded in 100-mm dishes (300–500,000 cells/dish) in H-5% NCS. Cells were cultured until 80% confluent, with media changes every 2 days. On the day of assay, cells were refed 10 ml/dish H-5% NCS. After 2 h, cells were washed with PBS, subjected to hypotonic shock, and scraped as described (20). Aliquots of 150 μl with ~200–250 μg cell protein were used per assay reaction. The reaction was initiated by the addition of 20 μl of [^{14}C]oleoyl-CoA (15 nmol; 30,000 dpm/nmol) containing 300 μg of BSA in 125 mM Tris-HCL, pH 7.8. Assays were carried out at 37°C for 3–15 min. Lipids were extracted and analyzed by TLC on silica gel 60 plates as described (21).

LDL receptor activity, and the esterification of LDL-derived [^{3}H]cholesterol

On day 0, cells were seeded into 6-well plates (25,000 cells/well) in H-5% NCS. On day 2, cells were fed H-5% NCS. On day 3, cells were washed in HBSS and fed H-5% LPDS. On day 4, cells were incubated for 6 h with either ^{125}I-LDL or [^{3}H]CL-LDL. The uptake and proteolytic degradation of ^{125}I-LDL was measured by incubating cells with 20 μg/ml ^{125}I-LDL in the absence and presence of 500 μg/ml of unlabeled LDL. After 6 h, the release of ^{125}I-monoiodotyrosine was quantified as described (15). Specific degradation was calculated by subtracting the value obtained in the presence of unlabeled LDL from that obtained in its absence. The uptake and lysosomal hydrolysis of [^{3}H]CL-LDL was measured by quantifying cell-associated [^{3}H]cholesteryl linoleate and [^{3}H]cholesterol as described previously (22). The amount of LDL-derived [^{3}H]cholesterol that was re-esterified by ACAT to form cholesteryl [^{3}H]oleate was also quantified as described previously (22).

Filipin fluorescence microscopy

On day 0, cells were seeded in 4-well Falcon 4104 chamber slides (1,500 cells/well) in H-5% NCS. On day 2, cells were refed. On day 3, cells were washed with PBS and processed for filipin fluorescence microscopy as described (23).

Cholesterol oxidase treatment

On day 0, cells were seeded into 6-well plates (25,000 cells/well) in H-5% NCS. On day 2, cells were washed in HBSS and fed H-5% LPDS. On day 3, cells were incubated in H-5% LPDS containing 20 μg/ml [^{3}H]CL-LDL. After 2 h, cells were treated with cholesterol oxidase, and the conversion of [^{3}H]cholesterol to [^{3}H]cholestenone was quantified as described (24).

Amphotericin B killing

On day 0, cells were seeded in 96-well plates (15,000 cells/well) in H-5% NCS. On day 1, cells were fed H-5% LPDS. On day 2, cells were fed H-5% LPDS/mev. After 8 h, cells were fed H-5% LPDS/mev with indicated additions of LDL. On day 3, cells were incubated 5 h in H-1% LPDS with or without 100 μg/ml amphotericin B. After 5 h, cells were washed with HBSS. Cell viability was assessed using a colorimetric 3-(4,5-dimethyl thiazol-2-yl)-2,5-diphenyl tetrazolium bromide (MTT) assay as described (22). Cell survival is defined as the mean MTT cleaved (A_{560}) per well from three wells treated with amphotericin B expressed as a percentage of the mean MTT cleaved (A_{560}) per well from three wells not treated with amphotericin B.

Basal esterification of plasma membrane cholesterol

On day 0, cells were seeded into 6-well plates (20,000 cells/well) in H-5% NCS. On day 2, cells were washed with HBSS and fed H-5% LPDS. Additions of 1.3 μCi/ml [^{3}H]cholesterol in ethanol were made at staggered times. On day 4, cells were washed with TBS. Lipids were extracted, separated, and quantified as described (22).

Movement of newly-synthesized cholesterol to the plasma membrane

Method 1. On day 0, cells were seeded in 6-well plates (25,000 cells/well) in H-5% NCS. On day 1, cells were washed with HBSS and fed H-5% LPDS. On day 3, cells were fed H-5% LPDS + 2% 2-hydroxypropyl-β-cyclodextrin. Additions of 60 μCi/ml [^{3}H]acetate were made at staggered times. At time of harvest, the media were removed and centrifuged. The supernatant was extracted with petroleum ether, and the upper phase containing the [^{3}H]cholesterol was removed and evaporated to dryness. Cell monolayers were washed once quickly, 2 × 7 min with TBS-BSA, and twice quickly with TBS. Cellular lipids were extracted using hexane-isopropyl alcohol (3:2, v/v). Monolayers were dissolved in 0.1 N NaOH, and aliquots were taken for protein determination. [^{3}H]cholesterol was isolated by TLC using heptane-ethyl ether (90:60, v/v). The endogenously labeled [^{3}H]sterols cochromatograph with authentic cholesterol; however, they can be resolved by HPLC into [^{3}H]cholesterol (70%) and [^{3}H]desmosterol (30%). They are referred to as [^{3}H]cholesterol.

Method 2. On day 0, cells were seeded in 6-well plates (25,000 cells/well) in H-5% NCS. On day 1, cells were washed with HBSS and fed H-5% LPDS. On day 3, cells were fed H-5% LPDS and additions of 60 μCi/ml [^{3}H]acetate were made at staggered times. At time of harvest, cells were treated with cholesterol oxidase, and the conversion of [^{3}H]cholesterol to [^{3}H]cholestenone was quantified as described (24).

Cholesterol content

On day 0, cells were seeded into 100-mm dishes (100,000 cells/dish) in H-5% NCS. On day 2, cells were washed with HBSS and fed H-5% NCS or H-5% LPDS. On day 4, cells were washed with TBS. Lipids were extracted and quantified as previously described (23), except that each sample consisted of one 100-mm dish. Gas chromatography was conducted isothermally using a DB-17 capillary column (15 m × 0.53 mm, Alltech) at 245°C.

Secretion of newly-synthesized proteins to the medium

Method 1. On day 0, cells were seeded in 6-well plates (50,000 cells/well) in H-5% NCS. On day 1, cells were refed 1 ml of Dulbecco's Modified Eagle Medium (no methionine, no cysteine) containing 10 mM ammonium chloride and 50 μCi EasyTag Express ^{35}S. At staggered times, the media were removed and centrifuged, and subjected to TCA precipitation. The pellets were dissolved in 0.5 N NaOH and subjected to liquid scintillation counting.

Method 2. On day 0, cells were seeded in 24-well plates (12,000 cells/well) in H-5% NCS. On day 1, cells were refed H-10% NCS with and without 20 μM 1-monopalmityl glyceryl ether (Doosan Serdary Research Laboratories). This compound is readily taken into cells, entering the pathway downstream of DHAPAT and alkyl-DHAP synthase. Incubation with this substrate over a period of 2–3 days restores PlsEtn levels to normal in NRel-4 cells (3). On day 4, cells were refed 200 μl of Dulbecco's Modified Eagle Medium (no methionine, no cysteine) after which staggered additions of EasyTag Express ^{35}S were made (50 μCi/well). At time of harvest, the media were removed and centrifuged. Aliquots were subjected to 12% SDS-PAGE, after which gels were fixed, impregnated with Autofluor (National Diagnostics), and exposed to film. Densitometric analysis was performed using an AlphaImager 2200.

Fluid-phase endocytosis and clearance of [^{14}C]sucrose

To measure endocytosis, on day 0, cells were seeded into 6-well dishes (50,000 cells/dish) in H-5% NCS. On day 1, cells were refed H-10% NCS with and without 20 μM 1-monopalmityl glyceryl ether. On day 4, [^{14}C]sucrose (260 μCi) was dried under nitrogen at 37°C and dissolved in 260 μl water. Cells were refed 1 ml of H-5% NCS after which staggered additions of 10 μCi [^{14}C]sucrose were made. At time of harvest, cells were washed with TBS containing 2 mg/ml BSA (once quickly, then six times, 3 min each), then with TBS (once quickly, then 5 min). Cells were solubilized with 1 ml 1% SDS for 30 min. Aliquots of the cell extract were subjected to liquid scintillation counting in 10 ml of ReadySafe and protein determination (19).

To measure clearance of endocytosed [^{14}C]sucrose, on day 0, cells were seeded in 6-well plates (25,000 cells/well) in H-5% NCS. On day 2, cells were refed H-5% NCS. [^{14}C]sucrose was dried under nitrogen at 37°C, dissolved in water, added to H-5% NCS, and stored at 4°C overnight. On day 3, cells were refed 0.5 ml H-5% NCS containing 70–200 μCi [^{14}C]sucrose. After 3 h, cells were washed six times with H-5% NCS and refed 1 ml H-5% NCS. At the indicated time, the media were removed and subjected to centrifugation (15,000 *g*, 5 min). Cells were washed with TBS containing 2 mg/ml BSA (once quickly, then 5 min), then with TBS (once quickly, then 5 min). Cells were solubilized with 1 ml 1% SDS for 30 min. Aliquots of media and cell extract were subjected to liquid scintillation counting in 10 ml of ReadySafe.

RESULTS

Plasmalogen biosynthesis

Plasmalogen synthesis begins in peroxisomes, where DHAPAT catalyzes the formation of acyl-DHAP (25) (**Fig. 1**). Alkyl-DHAP synthase catalyzes the second step in the pathway, forming the ether bond to produce alkyl-DHAP. Plasmalogen synthesis then continues in the ER. NRel-4 and NZel-1 cells are independently isolated CHO cell mutants defective in DHAPAT and alkyl-DHAP synthase, respectively (3, 14). Unlike other plasmalogen-deficient mutants (26, 27), NRel-4 and NZel-1 have single enzyme defects

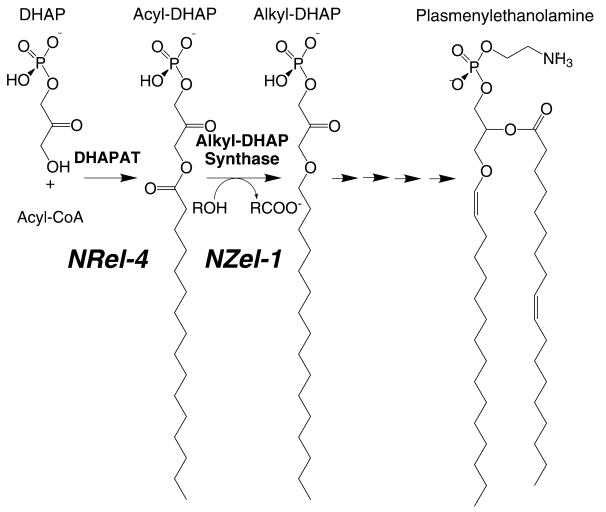

Fig. 1. Initial steps of plasmalogen biosynthesis. The first two steps of plasmalogen biosynthesis occur in peroxisomes. These two steps are shown, and the enzymes that are defective in the mutants used in this study, dihydroxyacetonephosphate acyltransferase (DHAPAT) and alkyl-dihydroxyacetone phosphate (DHAP) synthase, are indicated. The structure of plasmenylethanolamine is also included.

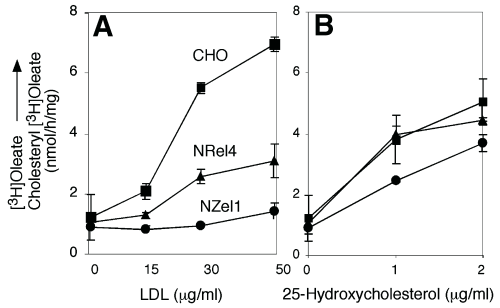

Fig. 2. Stimulation of cholesterol esterification by LDL (A) and by 25-hydroxycholesterol (B). Parental Chinese hamster ovary (CHO) (square), mutant NRel-4 (triangle), and mutant NZel-1 (circle) cells were grown as described in Experimental Procedures. On day 4, each monolayer received 1 ml of H-5% lipoprotein-deficient serum (LPDS) containing the indicated concentration of LDL or 25-hydroxycholesterol. After 5 h of incubation, cells were pulse labeled with 100 μM [^{3}H]oleate for 2 h. The cellular content of cholesterol [^{3}H]oleate was determined as described in Experimental Procedures. Data represent the mean ± SD of triplicate cultures.

and intact functional peroxisomes (3, 14). These cells make excellent model systems in which to study the relationship between plasmalogen and cholesterol metabolism. We were interested in investigating this relationship because of the apparent effect of plasmalogens on the pool of cellular cholesterol available for efflux to HDL (11). If plasmalogens play a role in membrane fission and fusion (9), a PlsEtn deficiency may alter cholesterol transport pathways throughout the cell.

Stimulation of cholesterol esterification by LDL and 25-hydroxycholesterol

ACAT is a resident ER enzyme (28) that catalyzes cholesterol esterification. ACAT activity is low when the ER cholesterol content is low and the enzyme is allosterically activated by cholesterol (29). The ability of LDL to stimulate ACAT activity depends on LDL receptor activity, hydrolysis of LDL's cholesteryl esters, and transport of LDL-derived cholesterol from lysosomes to the ER.

Figure 2 shows LDL (A) and 25-hydroxycholesterol (B) stimulation of cholesterol esterification in parental CHO, mutant NRel-4, and NZel-1 cells. Parental CHO cells incubated in the absence of LDL showed low rates of incorporation of [^{3}H]oleate into cholesteryl [^{3}H]oleate (1.2 nmol/h/mg). When LDL was added, cholesterol esterification was stimulated in a concentration-dependent manner such that 50 μg/ml LDL increased cholesterol esterification 6-fold. Mutant NRel-4 and NZel-1 cells also exhibited low rates of cholesterol esterification in the absence of LDL (1.1 and 0.9 nmol/h/mg, respectively); however, LDL stimulated cholesterol esterification only 3-fold and 2-fold, respectively. 25-Hydroxycholesterol stimulated cholesterol esterification equivalently in all cell lines, suggesting that ACAT is not defective in the mutant lines. Furthermore, in vitro ACAT activity was equivalent in CHO and NRel-4 cells at 7.97 ± 2.18 and 7.14 ± 0.8 pmol cholesteryl [^{14}C]oleate formed/min/mg protein, respectively (n = 3 experiments).

Is the blunted response to LDL due to a lack of PlsEtn? **Figure 3** shows LDL stimulation of cholesterol esterification in parental CHO cells and mutant NRel-4 cells that have been transfected with the control plasmid pBK-CMV (NRel-4/vector) or with the pBK-CMV plasmid containing the DHAPAT cDNA (NRel-4/DHAPAT). In parental CHO cells, LDL stimulated cholesterol esterification in a concentration-dependent manner, whereas LDL stimulation of cholesterol esterification was blunted in NRel-4 cells transfected with the control vector. However, in pDHAPAT-transfected NRel-4 cells, LDL-stimulated cholesterol esterification at wild-type levels. Thus, expression of pDHAPAT in NRel-4 cells corrected the aberrant LDL stimulation of cholesterol esterification.

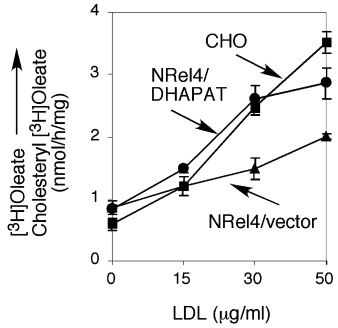

Fig. 3. LDL stimulation of cholesterol esterification in mutant cells transfected with the DHAPAT cDNA. Parental CHO (square), NRel-4 mock-transfected (triangle), and NRel-4 DHAPAT cDNA-transfected (circle) cells were grown as described in Experimental Procedures. On day 4, each monolayer received 1 ml of H-5% LPDS containing the indicated concentration of LDL. After 5 h of incubation, cells were pulse labeled with [^{3}H]oleate for 2 h. The cellular content of cholesterol [^{3}H]oleate was determined as described in Experimental Procedures. Data represent the mean ± SD of triplicate cultures.

TABLE 1. LDL receptor activity

	LDL Receptor Ligand	
	^{125}I-LDL Degradation	[^{3}H]CL-LDL Hydrolysis
	ng/mg protein	%
Cell line		
CHO	1137 ± 113	82 ± 6
NRel-4	1180 ± 423	82 ± 6

Cells were grown and analyzed as described in Experimental Procedures. Monolayers were incubated with either ^{125}I-LDL or [^{3}H]CL-LDL for 6 h. The amount of ^{125}I-LDL internalized and degraded was determined and is expressed as ng/mg cell protein. Data represent the mean ± SD of three experiments. The cellular content of [^{3}H]cholesterol (C), [^{3}H]cholesteryl linoleate (CL), and [^{3}H]cholesteryl oleate (CO) was analyzed. Hydrolysis of LDL-derived [^{3}H]CL is calculated as ([^{3}H]C+[^{3}H]CO)/([^{3}H]CL+[^{3}H]C+[^{3}H]CO) and is expressed as a percentage. Data represent the mean ± SD of four experiments.

LDL receptor activity and lysosomal storage of LDL-cholesterol

Defective LDL stimulation of cholesterol esterification could be explained by reduced LDL receptor activity or reduced hydrolysis of LDL-derived cholesteryl esters in lysosomes. We measured LDL receptor activity using ^{125}I-LDL as a LDL receptor ligand. CHO and NRel-4 cells were incubated for 6 h with 20 μg/ml ^{125}I-LDL and the amount of ^{125}I-LDL internalized and degraded was determined. **Table 1** shows that CHO and NRel-4 cells internalized and degraded similar amounts of ^{125}I-LDL. We next measured LDL-cholesteryl ester hydrolysis using [^{3}H]cholesteryl linoleate-labeled LDL as a receptor ligand. CHO and NRel-4 cells were incubated for 6 h in [^{3}H]CL-LDL after which cell-associated [^{3}H]cholesteryl esters and [^{3}H]cholesterol were quantified. Table 1 shows that the percentage of LDL cholesteryl esters hydrolyzed was the same in both cell types. This result indicates that defective LDL stimulation of cholesterol esterification in the mutant line is not a result of the mutant's inability to obtain free cholesterol from LDL.

Defective LDL stimulation of cholesterol esterification could also be explained by aberrant lysosomal sequestration of LDL-derived cholesterol, as is seen in NPC fibroblasts (30). Possible lysosomal storage of LDL-cholesterol (LDL-C) was assessed by culturing CHO and NRel-4 cells in LDL-containing medium, then examining filipin-stained cells by fluorescence microscopy. Filipin is a fluorescent polyene antibiotic that binds specifically to cholesterol and is used to detect cellular cholesterol pools. Wild-type CHO cells exhibited filipin staining at the plasma membrane and in a punctate distribution, most likely representing endosomes and lysosomes (**Fig. 4**). NRel-4 cells were indistinguishable from control cells, whereas CHO mutant 2-2 with the NPC phenotype (17) showed the characteristic lysosomal storage of free cholesterol.

These results indicated that reduced LDL-stimulation of cholesterol esterification was not due to lysosomal sequestration of LDL-C, but must result from defective post-lysosomal cholesterol transport to the ER. Thus, we next examined pathways of cholesterol transport in the plasmalogen-deficient mutant NRel-4.

Movement of LDL-derived cholesterol from lysosomes to the plasma membrane

The bulk of LDL-C that exits lysosomes is transported to the plasma membrane (31). This pathway was assessed using two approaches. First, the movement of LDL-derived [^{3}H]cholesterol to a cholesterol oxidase-sensitive pool was measured. Cells were incubated for 4 h with [^{3}H]CO-LDL, then treated with cholesterol oxidase using conditions under which only plasma membrane cholesterol is oxidized (22, 32). LDL-derived [^{3}H]cholesterol that has been transported to the plasma membrane will be oxidized to [^{3}H]cholestenone. **Table 2** shows that similar amounts of LDL-C were accessible to cholesterol oxidase in CHO and NRel-4 cells. In contrast, the NPC1-deficient mutant 2-2 showed significantly less [^{3}H]cholestenone formation, consistent with [^{3}H]cholesterol sequestration in lysosomes.

The second approach used to measure cholesterol transport along this pathway was to examine LDL-dependent amphotericin B killing of parental and mutant cells. Amphotericin B is a polyene antibiotic that forms aqueous

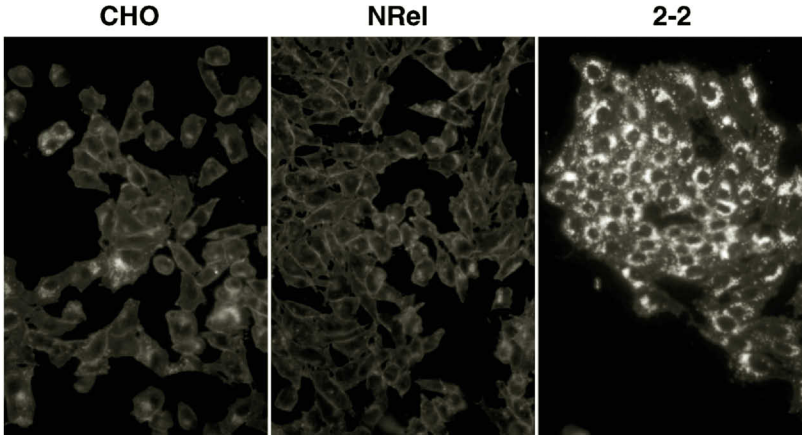

Fig. 4. Localization of cellular cholesterol. Parental CHO cells, plasmenyethanolamine (PlsEtn)-deficient NRel-4 cells, and Niemann-Pick disease type C (NPC)1-defective 2-2 cells were grown as described in Experimental Procedures. Cells were stained with filipin and examined by fluorescence microscopy.

TABLE 2. Quantification of the cholesterol-oxidase sensitive pool of cholesterol

	[^{3}H]cholestenone	
	Experiment 1	Experiment 2
	%	
Cell line		
CHO	45.3 ± 6.5	48.7 ± 9.0
NRel-4	42.0 ± 5.4	42.3 ± 11.4
2-2	27.1 ± 7.9	29.0 ± 4.2

Cells were grown as described in Experimental Procedures. Monolayers were incubated in H-5% LPDS containing 20 μg/ml [^{3}H]CO-LDL. After 4 h, cells were cholesterol oxidase-treated, and the conversion of [^{3}H]cholesterol to [^{3}H]cholestenone was quantified as described in Experimental Procedures. Data are expressed as the percentage of LDL-derived [^{3}H]cholesterol that has been oxidized to [^{3}H]cholestenone and are the average ± SD of three wells.

pores in cholesterol-rich membranes (33–35). Cells grown in conditions under which the plasma membrane is rich in synthesized or LDL-derived cholesterol are killed by amphotericin B. **Figure 5** illustrates LDL-dependent amphotericin B killing of CHO and NRel-4 cells. In this experiment, cells were incubated in media containing various concentrations of LDL for 16 h and treated with amphotericin B for 5 h. Cell survival was assessed using a colorimetric MTT assay. When cells were grown in H-5% NCS or H-5% LPDS, cell survival was low in both cell lines due to the arrival of endogenously synthesized cholesterol in the plasma membrane (data not shown). Cells cultured in H-5% LPDS/mev survived amphotericin B treatment because endogenous cholesterol synthesis was blocked by mevinolin. The addition of LDL caused concentration-dependent killing that was equivalent in both cell lines. This result further supports the idea that transport of cholesterol from lysosomes to the plasma membrane is normal in NRel-4 cells.

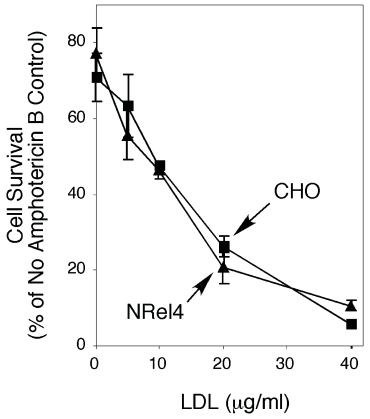

Fig. 5. LDL-dependent amphotericin B killing of normal and mutant cells. Parental CHO cells (square) and mutant NRel-4 cells (triangle) were grown as described in Experimental Procedures. Monolayers were incubated in H-5% LPDS/mev with the indicated concentration of LDL. After 16 h, monolayers were treated with amphotericin B, and cell viability was determined using a colorimetric 3-(4,5-dimethyl thiazol-2-yl)-2,5-diphenyl tetrazolium bromide (MTT) assay as described in Experimental Procedures. The data are expressed as the percentage of cells that survive amphotericin B treatment.

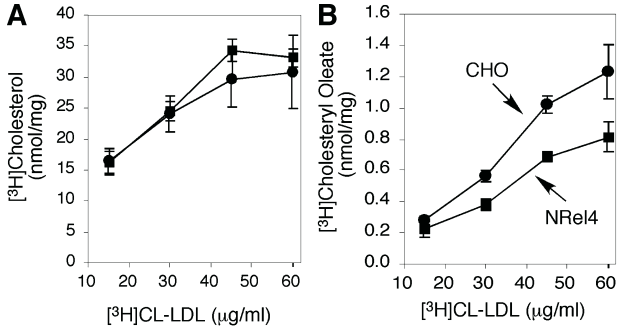

Fig. 6. Esterification of LDL-derived [^{3}H]cholesterol. Parental CHO (circle) and mutant NRel-4 (square) cells were grown as described in Experimental Procedures. Monolayers were incubated in H-5% LPDS/mev containing the indicated amount of LDL that is labeled with [^{3}H]cholesteryl linoleate ([^{3}H]CL-LDL) for 6 h. The amount of LDL-derived [^{3}H]cholesterol (A) and [^{3}H]cholesteryl oleate (B) was analyzed as described in Experimental Procedures. The data represent the mean ± SD of triplicate cultures.

Movement of LDL-derived cholesterol from lysosomes to ER

Approximately 30% of LDL-C that exits lysosomes is transported to ACAT in the ER by a pathway that is independent of the plasma membrane (22, 31). We investigated whether this pathway is normal in NRel-4 cells. Cells were incubated for 6 h with different amounts of [^{3}H]CL-LDL. For each concentration, we determined the amount of LDL-derived [^{3}H]cholesterol that was transported to ACAT and converted to [^{3}H]cholesteryl oleate (36). In this experiment, LDL receptor activity was equivalent in the two cell lines. **Figure 6A** shows the cellular content of [^{3}H]cholesterol after 6 h in the indicated amount of [^{3}H]CL-LDL. However, the amount of LDL-C that was transported to ACAT and re-esterified to cholesteryl oleate in NRel-4 cells was significantly reduced, at 63% of control levels (Fig. 6 B).

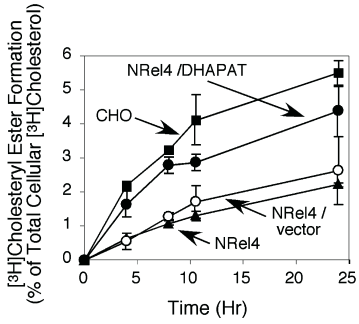

Fig. 7. Basal esterification of plasma membrane cholesterol. Parental CHO cells (square), mutant NRel-4 (triangle), NRel-4 transfected with control vector (circle), and NRel-4 transfected with pDHAPAT (circle) were grown and labeled as described in Experimental Procedures. Monolayers were incubated in H-5% LPDS containing [^{3}H]cholesterol for the indicated times. [^{3}H]cholesterol and [^{3}H]cholesteryl oleate were analyzed as described in Experimental Procedures. [^{3}H]cholesteryl oleate formation is expressed as a percentage of total cellular [^{3}H]cholesterol. The data represent the mean ± SD of triplicate cultures.

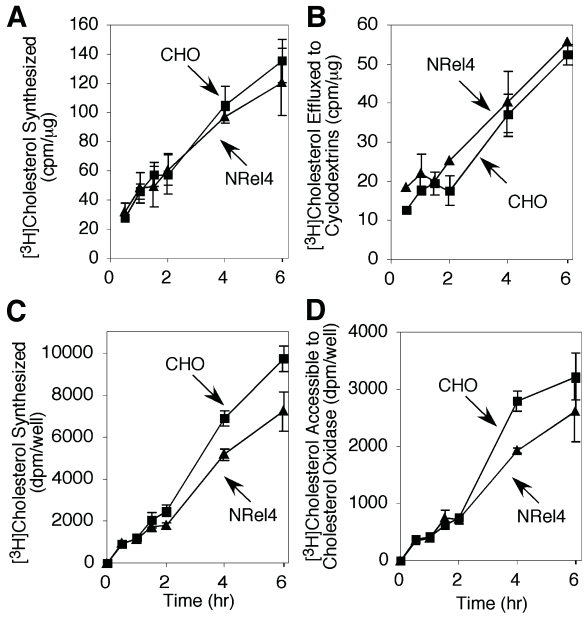

Fig. 8. Movement of newly-synthesized sterols to the plasma membrane. Parental CHO (square) and NRel-4 (triangle) cells were grown as described in Experimental Procedures. Sterol transport to the plasma membrane was assessed using two methods. Method 1: Monolayers were incubated in H-5% LPDS containing 2% cyclodextrin, and [^{3}H]acetate was added at various times. The medium (A) and total (B) content of [^{3}H]sterols was determined as described in Experimental Procedures. Method 2: Monolayers were incubated in H-5%LPDS and [^{3}H]acetate was added at various times. At time of harvest, the amount of [^{3}H]sterol synthesized (C) and [^{3}H]sterol accessible to cholesterol oxidase (D) was quantified as described in Experimental Procedures. Data represent the mean ± SD of triplicate cultures.

Plasma membrane to ER cholesterol transport

We evaluated basal cholesterol movement from the plasma membrane to the ER by incubating the cells for various times with [^{3}H]cholesterol (22). As seen in **Fig. 7**, CHO cells showed a time-dependent incorporation of [^{3}H]cholesterol into [^{3}H]cholesteryl ester, whereas NRel-4 cells esterified [^{3}H]cholesterol at 33% of control. NRel-4 cells transfected with control DNA (NRel-4/vector) had similar rates of esterification as NRel-4 cells, whereas NRel-4 cells transfected with pDHAPAT (NRel-4/DHAPAT) esterified [^{3}H]cholesterol at a rate similar to CHO cells. These results indicate that NRel-4 cells are defective in movement of plasma membrane cholesterol to the ER, and that this defect is a result of the PlsEtn deficiency.

Movement of newly-synthesized cholesterol to the plasma membrane

We evaluated the transport of newly-synthesized cholesterol from the ER to the plasma membrane by pulse-labeling cells for various times in [^{3}H]acetate. [^{3}H]cholesterol arrival in the plasma membrane was assessed using two approaches. First, we quantified the amount of [^{3}H]cholesterol capable of effluxing to cyclodextrins in the media (**Fig. 8A**, **B**). Throughout the time course, CHO cells efluxed 37 ± 5.6% of newly synthesized [^{3}H]cholesterol, whereas NRel-4 cells effluxed 45 ± 6.5%. Second, we quantified the amount of newly synthesized cholesterol that is accessible to cholesterol oxidase (Fig. 8C, D). Using this approach, 35 ± 4.7% of newly synthesized [^{3}H]cholesterol was accessible to cholesterol oxidase in CHO cells, and 38 ± 3.1% in NRel-4 cells. Thus, both methods show that NRel-4 cells synthesized and transported [^{3}H]cholesterol to the plasma membrane with normal kinetics.

Cellular cholesterol content

Our hypothesis is that the reduced LDL stimulation of esterification is the result of a reduced capacity of NRel-4 cells to transport cholesterol to ACAT in the ER. If this is correct, then the free cholesterol content of NRel-4 cells should be normal, but the cholesteryl ester content should be reduced. An alternative explanation is that NRel-4 cells have a lower cholesterol content than normal cells, and [^{3}H]cholesterol fills the depleted plasma membrane pool rather than moving to the ER. Thus, we have measured by gas-liquid chromatography the cholesterol and cholesteryl ester contents of CHO and NRel-4 cells that were cultured in H-5% NCS or H-5% LPDS (**Table 3**). CHO and NRel-4 cells grown in H-5% LPDS had similar cholesterol and cholesteryl ester contents. Growth in lipoprotein-containing H-5% NCS caused an equivalent increase in free cholesterol in both cell lines; however, there was a significantly higher increase in cholesteryl ester content in CHO cells compared with NRel-4 cells. This result is consistent with the LDL stimulation of cholesterol ester-

TABLE 3. Cellular levels of free and esterified cholesterol

Cell line	Medium	Cholesterol		
		Total	Free	Esterified
			μg/mg protein	
CHO	NCS	37.7 ± 3.6	29.2 ± 4.9	8.5 ± 1.5
NRel-4	NCS	29.5 ± 5.3	26.3 ± 4.6	3.2 ± 1.4[a]
C H O	LPDS	12.0 ± 1.6	11.7 ± 2.5	0.36 + 1.2
NRel-4	LPDS	9.5 ± 1.3	9.8 ± 1.8	0

Cells were grown as described in Experimental Procedures. Monolayers were grown for 2 days in H-5% NCS or H-5% LPDS. Cells were harvested and cholesterol was quantified as described in Experimental Procedures. Cholesterol content is reported as μg cholesterol per mg protein. Data represent the mean ± SD of three experiments.

[a] Significant difference ($P < .05$) when compared with CHO cells.

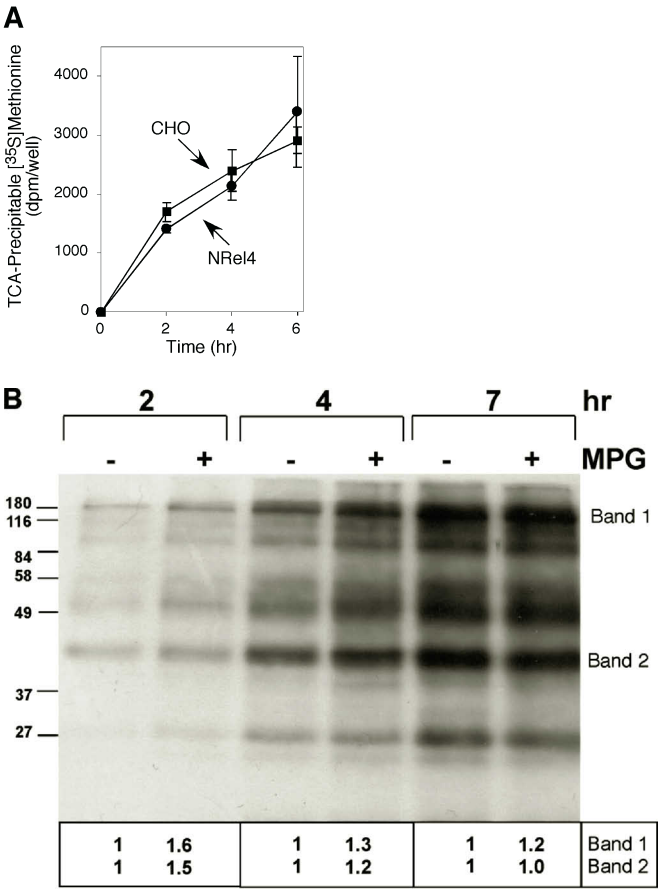

Fig. 9. Secretion of newly-synthesized proteins to the medium. Parental CHO (square) and NRel-4 (circle) cells were grown as described in Experimental Procedures. Cells were cultured for 2 days with and without 20 μM 1-monopalmityl glyceryl ether (MPG), then pulse-labeled with EasyTag Express ^{35}S (50 μCi/well). After the indicated time interval, levels of [^{35}S-containing protein in the media were quantified by TCA precipitation and liquid scintillation counting (A) or SDS-PAGE and densitometry (B) as described in Experimental Procedures. TCA-precipitable dpm/well represent the mean of triplicate cultures. Relative levels of high and low molecular weight bands are given.

ification shown in Fig. 2 and provides evidence that the lowered basal esterification is a result of a pathway defect rather than a lack of cholesterol available to move along that pathway.

Secretion of newly synthesized proteins to the medium

The cholesterol transport pathways that are affected by the lack of plasmalogens are vesicular pathways, based on the effects of pharmacological agents (37). Does the lack of PlsEtn reduce the flow of cholesterol along those transport pathways because they require efficient membrane fission and fusion? If so, then other vesicular transport pathways should be affected. Vesicular transport of proteins was compared in CHO and NRel-4 cells, and in NRel-4 cells and NRel-4 cells cultured for 2 days with 1-monopalmityl glyceryl ether, which enters the PlsEtn biosynthetic pathway downstream of the NRel-4 defect and restores plasmalogen levels to normal (3). Cells were radiolabeled for various times with [^{35}S]methionine and the arrival of newly synthesized and secreted proteins in the medium was assessed either by TCA precipitation of proteins followed by liquid scintillation counting, or by gel electrophoresis and fluorography. The incorporation of [^{35}S]methionine into cellular proteins was equivalent in CHO cells and NRel-4 cells cultured with and without 1-monopalmityl glyceryl ether (data not shown). Furthermore, the secretion of newly synthesized proteins was equivalent in CHO and NRel-4 cells (**Fig. 9A**). Figure 9B shows the comparison of proteins secreted from NRel-4 cells cultured with and without 1-monopalmityl glyceryl ether. There is a discernable increase in the secretion of newly synthesized proteins from NRel-4 cells supplemented with 1-monopalmityl glyceryl ether, as compared with unsupplemented cells. Densitometric analysis of two bands revealed a mean increase of 30%, indicating that the vesicular protein secretion pathway is partially dependent on PlsEtn.

Fluid-phase endocytosis and exocytosis

We used [^{14}C]sucrose as a fluid-phase marker to test if endocytosis is affected by the PlsEtn deficiency (**Fig. 10A**). We found that levels of cell-associated [^{14}C]sucrose increased linearly with time in both control and NRel-4 cells. The rate of [^{14}C]sucrose accumulation in NRel-4 cells was less that of control; however, this difference was not corrected by restoration of PlsEtn levels. This indicates that the variation in endocytosis is not due to altered PlsEtn levels. Fluid-phase exocytosis was assessed by allowing cells to internalize [^{14}C]sucrose then quantifying its retrograde transport from endocytic compartments to the medium (38). Figure 10B shows that the clearance of [^{14}C]sucrose from control and NRel-4 cells was equivalent. This result indicates that exocytosis is also PlsEtn independent.

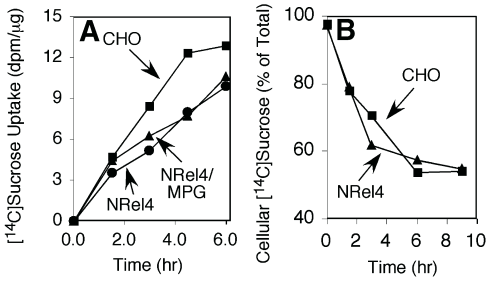

Fig. 10. Fluid-phase endocytosis and exocytosis. Parental CHO (square) and NRel-4 (circle) cells were grown as described in Experimental Procedures. Where indicated, NRel-4 cells were cultured for 2 days with 20 μM 1-monopalmityl glyceryl ether (MPG) (triangle). A: Monolayers were incubated in H-5% newborn calf serum (NCS) + [^{14}C]sucrose for the indicated amount of time, and cell-associated [^{14}C]sucrose was measured as described in Experiment Procedures. B: Monolayers were incubated in H-5% NCS + [^{14}C]sucrose for 3 h, washed extensively, and then incubated in H-5% NCS for the indicated amount of time. Cell-associated and medium radioactivity was quantified as described in Experiment Procedures. All data represent the mean of duplicate cultures.

DISCUSSION

Our work on plasmalogen's role in cholesterol transport was prompted by two recent findings. First, Mandel et al. (11) reported an effect of plasmalogens on HDL-mediated cholesterol efflux. Normal and plasmalogen-deficient murine macrophage-like RAW cells were labeled with [^{3}H]cholesterol, and then [^{3}H]cholesterol efflux to HDL was measured. They found that HDL-mediated cholesterol efflux was reduced in the plasmalogen-deficient lines in comparison to the normal cell lines, which would be consistent with a plasmalogen effect on the pool of cellular cholesterol available for efflux to HDL. Specifically, they observed that the maximal amount of cholesterol transferred was altered, whereas the rate of cholesterol efflux was unaffected by the lack of plasmalogens.

Second was a report that plasmalogen levels were reduced in brain tissue from the NPC mouse model (12), which likely results from the impaired peroxisomal function found in NPC brain. The NPC1 gene defect results in reduced transport of cholesterol, glycosphingolipids, and fluid phase constituents out of lysosomes and late endosomes (38, 39). It is not clear how an NPC1 defect leads to loss of peroxisomal activities, but the subsequent plasmalogen deficiency may further impair cellular cholesterol movement and be a contributing factor in NPC disease progression.

In this study, we found that two independently isolated CHO mutants bearing different lesions in the plasmalogen biosynthetic pathway displayed a decreased ability to transport LDL-derived or plasma membrane cholesterol to ACAT in the ER. The phenotype of DHAPAT-defective NRel-4 cells could be completely reversed by recovery of plasmalogen levels in these cells following transfection with the DHAPAT gene. The phenotype is not due to a requirement for PlsEtn in ACAT's lipid milieu, since ACAT was activated to normal levels by 25-hydroxycholesterol. Oxysterols, such as 25-hydroxycholesterol, diffuse readily throughout the cell and activate ACAT independently of specific cholesterol transport mechanisms. Normal 25-hydroxycholesterol stimulation of cholesterol esterification indicated that ACAT was normal in the mutant cells and that delivery of surrounding substrate is not an issue. Furthermore, the lack of LDL-stimulation of cholesterol esterification was not the result of reduced LDL receptor activity or lysosomal hydrolysis of LDL-cholesteryl ester, or aberrant lysosomal storage of cholesterol. Instead, it is likely due to reduced trafficking of cholesterol from lysosomes and plasma membrane to the ER (22, 37). Other cholesterol transport steps were normal in PlsEtn-deficient cells, as was protein secretion and fluid phase endocytosis and exocytosis.

The PlsEtn-deficient phenotype closely resembled that of CHO mutant 3-6, which was isolated in our hunt for NPC-like mutant CHO cells (23). The 3-6 mutation also causes defective mobilization of cholesterol from the plasma membrane to the ER but does not affect other cholesterol transport pathways. 25-Hydroxycholesterol stimulation of ACAT was normal in mutant 3-6, as it was in PlsEtn-deficient cells. However, our work also showed that the PlsEtn-deficient phenotype was clearly distinct from the 3-6 phenotype. Mutant 3-6 cells have normal PlsEtn levels (data not shown). They are resistant to amphotericin B when supplied with endogenously synthesized cholesterol, LDL, or cholesterol sulfate (23), whereas the PlsEtn-deficient cells were amphotericin B sensitive under those conditions.

Our current results are not in agreement with Thai et al. (40), who found impaired membrane traffic in plasmalogen-deficient cells. They interpreted collagen accumulation in DHAPAT-deficient cells as indicating impaired transit of proteins through the trans Golgi network, whereas we found normal secretion of nascent proteins. They also reported cholesterol accumulation in late endosomal/lysosomal compartments of mutant cells, as measured by filipin fluorescence microscopy, whereas we found no discernable cholesterol accumulation. They also found diminished transferrin uptake and structurally altered caveolae and coated pits. We have not measured transferrin uptake but did find normal LDL internalization. Some of these differences may be due to the different cell models examined, i.e., human fibroblasts versus CHO cells. Other differences may not be related to the plasmalogen deficiency. Thai et al. (40) do not report the effect of restoration of plasmalogen levels on any of the phenotypic changes.

Mandel et al. (11) found diminished cholesterol efflux from plasmalogen-deficient murine RAW macrophages and human skin fibroblasts to the extracellular acceptor HDL, whereas we found no effect of plasmalogens on the movement of newly synthesized [^{3}H]sterol to the plasma membrane and efflux to cyclodextrin. The inconsistency between our results and those of Mandel et al. (11) likely arise from the different methods used to measure this process. Cyclodextrins have been shown to have a much higher efficiency in stimulating cholesterol efflux than HDL (41), and the cyclodextrin-accessible pool of cholesterol is likely to be different than the HDL accessible pool.

The question that we now face is what role does PlsEtn play in cholesterol movement to ACAT? Studies of plasmalogens in intact cells (10) and model systems (42) have shown that they have a role in protecting cells from oxidative damage. Plasmalogens are also thought to serve as sources of lipid mediators, such as arachidonic acid, that are involved in signal transduction (43). In addition, when PlsEtn is hydrolyzed by the plasmalogen-selective PLA_2, the lysoplasmalogen generated from the reaction can induce the synthesis of platelet-activating factor (44). However, it is difficult to rationalize how these putative functions would relate to cholesterol transport.

Another characteristic of PlsEtn is their ability to form non-bilayer structures. Studies of model membrane systems have shown that, like phosphatidylethanolamine, PlsEtn is a nonbilayer-forming phospholipid. However, the phase behavior of PlsEtn differs markedly from the related alkylacyl and diacyl species, with a liquid crystalline to inverse hexagonal transition temperature for the three species at 30°C, 53°C, and 68°C, respectively (9). Therefore, PlsEtn is the only one of these phospholipid species to form non-bilayer structures at or below physiological temperatures. The vinyl

ether bond causes PlsEtn to form a hexagonal array more readily than phosphatidyl-ethanolamine and, thus, they are hypothesized to play a role in membrane fission and fusion events (9, 45). In support of this, Glaser and Gross (45) showed that PlsEtn stimulated the kinetics of in vitro membrane fusion 6-fold when vesicles of physiologic phospholipid composition were compared with those in which PlsEtn was replaced with phosphatidylethanolamine. Does the PlsEtn deficiency in NRel-4 cells affect membrane fission or fusion? Our data are not consistent with this hypothesis as vesicle trafficking was normal by all criteria examined.

Future work must determine the precise role that plasmalogens have in this specific cholesterol transport pathway. We have not ruled out the idea that it is a product of phospholipase A_2 hydrolysis of PlsEtn rather than PlsEtn itself that is needed for cholesterol transport. The availability of the plasmalogen-deficient cell lines and our ability to modulate plasmalogen levels in those cells will allow us to examine and answer plasmalogen's role in cholesterol transport.

This work was supported by grants to L.L. from the National Institutes of Health (DK-49564) and Ara Parseghian Medical Research Foundation, and by a grant to R.A.Z. from the National Institutes of Health (GM-50571). The authors thank Wilhelm Just (University of Heidelberg, Germany) for providing the human DHAPAT cDNA and Catherine C. Y. Chang (Dartmouth Medical School) for assistance with the in vitro ACAT protocol. We also thank Margery Beinfeld (Tufts University School of Medicine) for assistance with LDL iodination.

REFERENCES

1. Nagan, N., and R. A. Zoeller. 2001. Plasmalogens: biosynthesis and functions. *Prog. Lipid Res.* **40:** 199–229.
2. Horrocks, L. A., and M. Sharma. 1982. Plasmalogens and *O*-alkyl glycerophospholipids. *In* Phospholipids J. N. Hawthorne and G. B. Ansell, editors. Elsevier, Amsterdam. 51–92.
3. Nagan, N., A. K. Hajra, L. K. Larkins, P. Lazarow, P. E. Purdue, W. B. Rizzo, and R. A. Zoeller. 1998. Isolation of a Chinese hamster fibroblast variant defective in dihydroxyacetonephosphate acyltransferase activity and plasmalogen biosynthesis: use of a novel two-step selection protocol. *Biochem. J.* **332:** 273–279.
4. Zoeller, R. A., and C. R. Raetz. 1992. Strategies for isolating somatic cell mutants defective in lipid biosynthesis. *Methods Enzymol.* **209:** 34–51.
5. Koizumi, K., S. Shimizu, K. T. Koizumi, K. Nishida, C. Sato, K. Ota, and N. Yamanaka. 1981. Rapid isolation and lipid characterization of plasma membranes from normal and malignant lymphoid cells of mouse. *Biochim. Biophys. Acta.* **649:** 393–403.
6. Breckenridge, W. C., I. G. Morgan, J. P. Zanetta, and G. Vincendon. 1973. Adult rat brain synaptic vesicles. II. Lipid composition. *Biochim. Biophys. Acta.* **320:** 681–686.
7. Bjerrum, O. W., H. Nielsen, and N. Borregaard. 1989. Quantitative analysis of phospholipids and demonstration of plasmalogen in human neutrophil subcellular fractions by high-performance liquid chromatography. *Scand. J. Clin. Lab. Invest.* **49:** 613–622.
8. Fellmann, P., P. Herve, and P. F. Devaux. 1993. Transmembrane distribution and translocation of spin-labeled plasmalogens in human red blood cells. *Chem. Phys. Lipids.* **66:** 225–230.
9. Lohner, K. 1996. Is the high propensity of ethanolamine plasmalogens to form non-lamellar lipid structures manifested in the properties of biomembranes? *Chem. Phys. Lipids.* **81:** 167–184.
10. Zoeller, R. A., A. C. Lake, N. Nagan, D. P. Gaposchkin, M. A. Legner, and W. Lieberthal. 1999. Plasmalogens as endogenous antioxidants: somatic cell mutants reveal the importance of the vinyl ether. *Biochem. J.* **338:** 769–776.
11. Mandel, H., R. Sharf, M. Berant, R. J. Wanders, P. Vreken, and M. Aviram. 1998. Plasmalogen phospholipids are involved in HDL-mediated cholesterol efflux: insights from investigations with plasmalogen-deficient cells. *Biochem. Biophys. Res. Commun.* **250:** 369–373.
12. Schedin, S., P. J. Sindelar, P. Pentchev, U. Brunk, and G. Dallner. 1997. Peroxisomal impairment in Niemann-Pick type C disease. *J. Biol. Chem.* **272:** 6245–6251.
13. Liscum, L. 2000. Niemann-Pick type C mutations cause lipid traffic jam. *Traffic.* **1:** 218–225.
14. Nagan, N., A. K. Hajra, A. K. Das, H. W. Moser, A. Moser, P. Lazarow, P. E. Purdue, and R. A. Zoeller. 1997. A fibroblast cell line defective in alkyl-dihydroxyacetone phosphate synthase: a novel defect in plasmalogen biosynthesis. *Proc. Natl. Acad. Sci. USA.* **94:** 4475–4480.
15. Goldstein, J. L., S. K. Basu, and M. S. Brown. 1983. Receptor-mediated endocytosis of low-density lipoprotein in cultured cells. *Methods Enzymol.* **98:** 241–260.
16. Faust, J. R., J. L. Goldstein, and M. S. Brown. 1977. Receptor-mediated uptake of low density lipoprotein and utilization of its cholesterol for steroid synthesis in cultured mouse adrenal cells. *J. Biol. Chem.* **252:** 4861–4871.
17. Dahl, N. K., K. L. Reed, M. A. Daunais, J. R. Faust, and L. Liscum. 1992. Isolation and characterization of Chinese hamster ovary cells defective in the intracellular metabolism of LDL-derived cholesterol. *J. Biol. Chem.* **267:** 4889–4896.
18. Liscum, L., and J. R. Faust. 1989. The intracellular transport of low density lipoprotein-derived cholesterol is inhibited in Chinese hamster ovary cells cultured with 3-b-[2-(diethylamino)ethoxy]androst-5-en-17-one. *J. Biol. Chem.* **264:** 11796–11806.
19. Lowry, O. H., N. J. Rosebrough, A. L. Farr, and R. J. Randall. 1951. Protein measurement with the Folin phenol reagent. *J. Biol. Chem.* **193:** 265–275.
20. Chang, T. Y., J. S. Limanek, and C. C. Chang. 1981. A simple and efficient procedure for the rapid homogenization of cultured animal cells grown in monolayer. *Anal. Biochem.* **116:** 298–302.
21. Chang, C. C. Y., G. M. Doolittle, and T. Y. Chang. 1986. Cycloheximide sensitivity in regulation of acyl coenzyme A:cholesterol acyltransferase activity in chinese hamster ovary cells. 1. Effect of exogenous sterols. *Biochemistry.* **25:** 1693–1699.
22. Underwood, K. W., N. L. Jacobs, A. Howley, and L. Liscum. 1998. Evidence for a cholesterol transport pathway from lysosomes to endoplasmic reticulum that is independent of the plasma membrane. *J. Biol. Chem.* **273:** 4266–4274.
23. Jacobs, N. L., B. Andemariam, K. W. Underwood, K. Panchalingam, D. Sternberg, M. Kielian, and L. Liscum. 1997. Analysis of a Chinese hamster ovary cell mutant with defective mobilization of cholesterol from the plasma membrane to the endoplasmic reticulum. *J. Lipid Res.* **38:** 1973–1987.
24. Porn, M. I., and J. P. Slotte. 1990. Reversible effects of sphingomyelin degradation on cholesterol distribution and metabolism in fibroblasts and transformed neuroblastoma cells. *Biochem. J.* **271:** 121–126.
25. Lee, T. C. 1998. Biosynthesis and possible biological functions of plasmalogens. *Biochim. Biophys. Acta.* **1394:** 129–145.
26. Zoeller, R. A., and C. R. Raetz. 1986. Isolation of animal cell mutants deficient in plasmalogen biosynthesis and peroxisome assembly. *Proc. Natl. Acad. Sci. USA.* **83:** 5170–5174.
27. Fujiki, Y. 1997. Molecular defects in genetic diseases of peroxisomes. *Biochim. Biophys. Acta.* **1361:** 235–250.
28. Chang, C. C. Y., J. Chen, M. A. Thomas, D. Cheng, V. A. D. Priore, R. S. Newton, M. E. Pape, and T-Y. Chang. 1995. Regulation and immunolocalization of acyl-coenzyme A:cholesterol acyltransferase in mammalian cells as studied with specific antibodies. *J. Biol. Chem.* **49:** 29532–29540.
29. Cheng, D., C. C. Y. Chang, X-m. Qu, and T.-Y. Chang. 1995. Activation of acyl-coenzyme A:cholesterol acyltransferase by cholesterol or by oxysterol in a cell-free system. *J. Biol. Chem.* **270:** 685–695.
30. Blanchette-Mackie, E. J., N. K. Dwyer, L. M. Amende, H. S. Kruth, J. D. Butler, J. Sokol, M. E. Comly, M. T. Vanier, J. T. August, R. O. Brady, and P. G. Pentchev. 1988. Type-C Niemann-Pick disease: low density lipoprotein uptake is associated with premature cholesterol accumulation in the Golgi complex and excessive cholesterol storage in lysosomes. *Proc. Natl. Acad. Sci. USA.* **85:** 8022–8026.
31. Neufeld, E. B., A. M. Cooney, J. Pitha, E. A. Dawidowicz, N. K. Dwyer, P. G. Pentchev, and E. J. Blanchette-Mackie. 1996. Intracellular

trafficking of cholesterol monitored with a cyclodextrin. *J. Biol. Chem.* **271:** 21604–21613.
32. Slotte, J. P., G. Hedstrom, S. Rannstrom, and S. Ekman. 1989. Effects of sphingomyelin degradation on cell cholesterol oxidizability and steady-state distribution between the cell surface and the cell interior. *Biochim. Biophys. Acta.* **985:** 90–96.
33. Kinsky, S. C. 1970. Antibiotic interaction with model membranes. *Annu. Rev. Pharmacol.* **10:** 119–142.
34. Norman, A. W., R. A. Demel, B. De Kruyeff, and L. L. M. Van Deenen. 1972. Studies on the biological properties of polyene antibiotics. Evidence for the direct interaction of filipin with cholesterol. *J. Biol. Chem.* **247:** 1918–1929.
35. De Kruijff, B. 1990. Cholesterol as a target for toxins. *Biosci. Rep.* **10:** 127–130.
36. Cadigan, K. M., D. M. Spillane, and T-Y. Chang. 1990. Isolation and characterization of Chinese hamster ovary cell mutants defective in intracellular low density lipoprotein-cholesterol trafficking. *J. Cell Biol.* **110:** 295–308.
37. Liscum, L., and N. J. Munn. 1999. Intracellular cholesterol transport. *Biochim. Biophys. Acta.* **1438:** 19–37.
38. Neufeld, E. B., M. Wastney, S. Patel, S. Suresh, A. M. Cooney, N. K. Dwyer, C. F. Roff, K. Ohno, J. A. Morris, E. D. Carstea, J. P. Incardona, J. F. Strauss 3rd, M. T. Vanier, M. C. Patterson, R. O. Brady, P. G. Pentchev, and E. J. Blanchette-Mackie. 1999. The Niemann-Pick C1 protein resides in a vesicular compartment linked to retrograde transport of multiple lysosomal cargo. *J. Biol. Chem.* **274:** 9627–9635.
39. Puri, V., R. Watanabe, M. Dominguez, X. Sun, C. L. Wheatley, D. L. Marks, and R. E. Pagano. 1999. Cholesterol modulates membrane traffic along the endocytic pathway in sphingolipid storage diseases. *Nat. Cell Biol.* **1:** 386–388.
40. Thai, T. P., C. Rodemer, A. Jauch, A. Hunziker, A. Moser, K. Gorgas, and W. W. Just. 2001. Impaired membrane traffic in defective ether lipid biosynthesis. *Hum. Mol. Genet.* **10:** 127–136.
41. Kilsdonk, E. P. C., P. G. Yancey, G. W. Stoudt, F. W. Bangerter, W. J. Johnson, M. C. Phillips, and G. H. Rothblat. 1995. Cellular cholesterol efflux mediated by cyclodextrins. *J. Biol. Chem.* **270:** 17250–17256.
42. Reiss, D., K. Beyer, and B. Engelmann. 1997. Delayed oxidative degradation of polyunsaturated diacyl phospholipids in the presence of plasmalogen phospholipids in vitro. *Biochem. J.* **323:** 807–814.
43. Ford, D. A., and R. W. Gross. 1989. Plasmenylethanolamine is the major storage depot for arachidonic acid in rabbit vascular smooth muscle and is rapidly hydrolyzed after angiotensin II stimulation. *Proc. Natl. Acad. Sci. USA.* **86:** 3479–3483.
44. Nieto, M. L., M. E. Venable, S. A. Bauldry, D. G. Greene, M. Kennedy, D. A. Bass, and R. L. Wykle. 1991. Evidence that hydrolysis of ethanolamine plasmalogens triggers synthesis of platelet-activating factor via a transacylation reaction. *J. Biol. Chem.* **266:** 18699–18706.
45. Glaser, P. E., and R. W. Gross. 1994. Plasmenylethanolamine facilitates rapid membrane fusion: a stopped-flow kinetic investigation correlating the propensity of a major plasma membrane constituent to adopt an HII phase with its ability to promote membrane fusion. *Biochemistry.* **33:** 5805–5812.